NEW MEASUREMENTS OF THE η and K^0 MASSES

The NA48 Collaboration

A. Lai, D. Marras
Dipartimento di Fisica dell'Università e Sezione dell'INFN di Cagliari, I-09100 Cagliari, Italy

J.R. Batley, A.J. Bevan[1], R.S. Dosanjh, T.J. Gershon[2], G.E. Kalmus, C. Lazzeroni, D.J. Munday, E. Olaiya, M.A. Parker, T.O. White, S.A. Wotton
Cavendish Laboratory, University of Cambridge, Cambridge, CB3 0HE, UK[3]

G. Barr, G. Bocquet, A. Ceccucci, T. Cuhadar-Dönszelmann, D. Cundy, G. D'Agostini, N. Doble, V. Falaleev, W. Funk, L. Gatignon, A. Gonidec, B. Gorini, G. Govi, ,P. Grafström, W. Kubischta, A. Lacourt, M. Lenti[4], I. Mikulec[5], A. Norton, S. Palestini, B. Panzer-Steindel, D. Schinzel, G. Tatishvili[6], H. Taureg, M. Velasco, H. Wahl
CERN, CH-1211 Geneva 23, Switzerland

C. Cheskov P. Hristov, V. Kekelidze, D. Madigojine, N. Molokanova, Yu. Potrebenikov, A. Zinchenko
Joint Institute for Nuclear Research, Dubna, Russian Federation

V.J. Martin[7], P. Rubin[8], R. Sacco, A. Walker
Department of Physics and Astronomy, University of Edinburgh, JCMB King's Buildings, Mayfield Road, Edinburgh, EH9 3JZ, UK[3)]

D. Bettoni, R. Calabrese, M. Contalbrigo, P. Dalpiaz, J. Duclos, P.L. Frabetti[9], A. Gianoli, E. Luppi, M. Martini, L. Masetti, F. Petrucci, M. Savrié, M. Scarpa
Dipartimento di Fisica dell'Università e Sezione dell'INFN di Ferrara, I-44100 Ferrara, Italy

[1] Present address: Oliver Lodge Laboratory, University of Liverpool, Liverpool L69 7ZE, U.K.

[2] Present address: High Energy Accelerator Research Organization (KEK), Tsukuba, Ibaraki, 305-0801, Japan

[3]Funded by the UK Particle Physics and Astronomy Research Council

[4] On leave from Sezione dell'INFN di Firenze, I-50125, Firenze, Italy

[5] On leave from Österreichische Akademie der Wissenschaften, Institut für Hochenergiephysik, A-1050 Wien, Austria

[6] On leave from Joint Institute for Nuclear Research, Dubna, 141980, Russian Federation

[7] Permanent address: Department of Physics and Astronomy, Northwestern University, 2145 Sheridan Road, Evanston IL 60202, USA

[8] Permanent address: Department of Physics, University of Richmond, VA 27313, USA

[9] Permanent address: Dipartimento di Fisica dell'Università e Sezione dell'INFN di Bologna, I-40126 Bologna, Italy

A. Bizzeti[10], M. Calvetti, G. Collazuol, G. Graziani, E. Iacopini, F. Martelli[11], M. Veltri[11)]
Dipartimento di Fisica dell'Università e Sezione dell'INFN di Firenze, I-50125 Firenze, Italy

H.G. Becker, M. Eppard, H. Fox, A. Hirstius, K. Holtz, A. Kalter, K. Kleinknecht, U. Koch, L. Köpke, P. Lopes da Silva, P. Marouelli, I. Mestvirishvili, I. Pellmann, A. Peters, S.A. Schmidt, V. Schönharting, Y. Schué, R. Wanke, A. Winhart, M. Wittgen
Institut für Physik, Universität Mainz, D-55099 Mainz, Germany[12]

J.C. Chollet, L. Fayard, L. Iconomidou-Fayard, J. Ocariz, G. Unal, I. Wingerter-Seez
Laboratoire de l'Accélérateur Linéaire, IN2P3-CNRS, Université de Paris-Sud, F-91405 Orsay, France[13]

G. Anzivino, P. Cenci, E. Imbergamo, G. Lamanna, P. Lubrano, A. Mestvirishvili, A. Nappi, M. Pepe, M. Piccini,
Dipartimento di Fisica dell'Università e Sezione dell'INFN di Perugia, I-06100 Perugia, Italy

R. Casali, C. Cerri, M. Cirilli[14], F. Costantini, R. Fantechi, L. Fiorini, S. Giudici, I. Mannelli, G. Pierazzini, M. Sozzi
Dipartimento di Fisica dell'Università, Scuola Normale Superiore e Sezione dell'INFN di Pisa, I-56100 Pisa, Italy

J.B. Cheze, J. Cogan, M. De Beer, P. Debu, F. Derue, A. Formica, G. Gouge, R. Granier de Cassagnac, G. Marel, E. Mazzucato, B. Peyaud, R. Turlay, B. Vallage
DSM/DAPNIA - CEA Saclay, F-91191 Gif-sur-Yvette, France

M. Holder, A. Maier, M. Ziolkowski
Fachbereich Physik, Universität Siegen, D-57068 Siegen, Germany[15]

R. Arcidiacono, C. Biino, N. Cartiglia, R. Guida, F. Marchetto, E. Menichetti, N. Pastrone

[10] Also at Dipartimento di Fisica dell'Università di Modena, I-41100 Modena, Italy
[11] Instituto di Fisica Universitá di Urbino
[12]Funded by the German Federal Minister for Research and Technology (BMBF) under contract 7MZ18P(4)-TP2
[13]Funded by Institut National de Physique des Particules et de Physique Nucléaire (IN2P3), France
[14] Present address: Dipartimento di Fisica dell'Universitá di Roma "La Sapienza" e Sezione INFI di Roma, I-00185 Roma, Italy
[15]Funded by the German Federal Minister for Research and Technology (BMBF) under contract 056SI74

Dipartimento di Fisica Sperimentale dell'Università e Sezione dell'INFN di Torino,
I-10125 Torino, Italy

J. Nassalski, E. Rondio, M. Szleper, W. Wislicki, S. Wronka
Soltan Institute for Nuclear Studies, Laboratory for High Energy Physics, PL-00-681 Warsaw, Poland[16]

H. Dibon, M. Jeitler, M. Markytan, G. Neuhofer, M. Pernicka, A. Taurok, L. Widhalm
Österreichische Akademie der Wissenschaften, Institut für Hochenergiephysik, A-1050 Wien, Austria[17]

Abstract

New measurements of the η and K^0 masses have been performed using decays to $3\pi^0$ with the NA48 detector at the CERN SPS. Using symmetric decays to reduce systematic effects, the results $M(\eta) = 547.843 \pm 0.051$ MeV/c^2 and $M(K^0) = 497.625 \pm 0.031$ MeV/c^2 were obtained.

Introduction

Precise values of the η and K^0 masses are often used as input for measurements. For instance, η decays involving photons are used for the precise in situ calibration of electromagnetic calorimeters. One such example is the measurement of the CP violating quantity ϵ'/ϵ performed by NA48 [1]. The current world average [2] relative uncertainty on the K^0 mass is $\pm 6 \times 10^{-5}$, dominated by a measurement at a ϕ factory using $\pi^+\pi^-$ decays [3]. The η mass is less well known, the current uncertainty being $\pm 2 \times 10^{-4}$. The most precise results in this case come from measurements of the production cross-section near threshold in the reactions $dp \to \eta^3He$ [4] and in $\gamma p \to \eta p$ [5].

In this paper, we present new measurements of the η and K^0 masses using decays to $3\pi^0$ ($\to 6\gamma$), with the NA48 experiment at the CERN SPS. The paper is organised as follows: the first section describes the method used for the reconstruction of the η and K^0 masses; the second section shows

[16] Supported by the Committee for Scientific Research grants 5P03B10120, 2P03B11719 and SPUB-MCERNP03DZ2102000 and using computing resources of the Interdisciplinary Center for Mathematical and Computational Modelling of the University of Warsaw

[17] Funded by the Austrian Ministry for Traffic and Research under the contract GZ 616.360/2-IV GZ 616.363/2-VIII, Austria and by the Fonds für Wissenschaft und Forschung FWF Nr. P08929-PHY

the experimental setup; details of the performances of the electromagnetic calorimeter are given in the third section; results and cross-checks with a detailed evaluation of the systematic effects are presented in the fourth section.

1 Method

This measurement uses η and K_L particles with average energies of ≈ 110 GeV. Photons from $3\pi^0$ decays are detected with a precise quasi-homogeneous liquid krypton calorimeter. This device allows photon energies as well as impact positions in the plane orthogonal to the η and K_L momentum to be measured accurately. Although photon angles are not measured directly with the calorimeter, the decay position can be inferred from two photons coming from a π^0 decay using the π^0 mass constraint. In the limit of small opening angles (valid to better than 10^{-5} for this experiment), the distance d between the decay position and the calorimeter nominal position can be computed as

$$d = \frac{1}{M_{\pi^0}} \sqrt{E_1 E_2} d_{12}$$

where M_{π^0} is the π^0 mass, known with 4×10^{-6} accuracy[2], E_1 and E_2 are the energies of the two photons from a π^0 decay and d_{12} is the distance between the two photons in the plane orthogonal to the beam axis at the calorimeter nominal position. Using the average value d_{π^0} of d from the three π^0 mass constraints, the full 6-body invariant mass can then be computed as

$$M = \frac{1}{d_{\pi^0}} \sqrt{\Sigma_{ij, i<j} E_i E_j d_{ij}^2}$$

The advantages of using this method for the mass measurement are the following:

- The $3\pi^0$ decay mode is virtually background free.
- Thanks to the π^0 mass constraint, the resolution on M is better than 1 MeV/c^2.
- The measurement of M is independent of the energy scale of the calorimeter. Indeed, the measured quantity is the ratio of the η (or K^0) mass to the π^0 mass, in which the absolute energy scale completely cancels. For the same reason, the absolute transverse size scale also cancels.

- The measurement is only sensitive to residual non-linearities in the energy or position measurements. To minimise the sensitivity to energy non-linearities, only symmetric decays are used, in which the photons all have about the same energy. Indeed for perfectly symmetric decay, the sensitivity to energy non-linearities also cancels .

- The same method can be applied to both the η and the K_L cases. The very large statistics available in the K_L sample allows many systematic cross-checks to be performed to validate the measurement.

The mass measurement relies only on measurements of relative distance between photons and ratio of energies with the calorimeter. Furthermore the performance of this device can be studied in detail in situ using K_{e3} ($K_L \to \pi^{\pm} e^{\mp} \nu$) decays, and π^0 and η decays to two photons, which are present with very large statistics in the data samples.

2 Beam and detectors

The NA48 experiment is designed for a precise measurement of the quantity ϵ'/ϵ in neutral kaon decays [1]. In the following only the parts of the apparatus relevant for the measurements of the η and K^0 masses are described.

2.1 The K_L beam

The neutral K_L beam [6] is derived from 450 GeV/c protons extracted from the CERN SPS. For each SPS pulse (2.4 s spill every 14.4 s), 1.5×10^{12} protons hit a 40 cm long beryllium target, with an incidence angle of 2.4 mrad. The charged component of the outgoing particles is swept away by bending magnets. A neutral secondary beam with a ± 0.15 mrad divergence is generated using three stages of collimation over 126 m, the final element being located just upstream of the beginning of the decay region. Because of the long distance between the target and the beginning of the decay region, the decays in this neutral beam are dominated by K_L. The decay region is contained in an evacuated ($< 3 \times 10^{-5}$ mbar) 90 m long tank. During the 1999 data taking, this decay region was terminated by a polyimide (Kevlar) composite window 0.9 mm (0.003 radiation lengths) thick. Downstream of it a 16 cm diameter evacuated tube passes through all detector elements to allow the undecayed neutral beam to travel in vacuum all the way to a beam dump. In the normal ϵ'/ϵ data taking, a K_S beam is also created using a second target closer to the decay region. The beam from which the decays originate is identified by tagging the protons directed to the K_S target.

2.2 The η beam

During special data taking periods, a beam of negatively charged secondary particles is, by a suitable choice of the magnets in the beam line, directed along the nominal K_L beam axis. This beam consists mostly of π^- with a broad momentum spectrum of average energy$\approx$ 100 GeV, and with a flux of $\approx 1.3 \times 10^6$ per pulse. It impinges on two thin polyethylene targets (2.0 cm thick), separated by 1462 cm, near the beginning and towards the end of the fiducial Kaon decay region. Through charge exchange reactions, π^0 and η are created and, because of their very short lifetimes, decay inside the targets. Neutral Kaon are also produced in the targets, mostly from K^- interactions.

2.3 The detector

The layout of the detector is shown in Figure 1. A magnetic spectrometer [7], housed in a helium tank, is used to measure charged particles. It is comprised of four drift chambers and a dipole magnet, located between the second and the third drift chambers, giving a horizontal transverse momentum kick of 265 MeV/c. The momentum resolution is $\sigma_p/p = 0.5\% \oplus 0.009\% \times p$ (p in GeV/c), where $\oplus$ means that the contributions should be added in quadrature. Two plastic scintillator hodoscope planes are placed after the helium tank.

A quasi-homogeneous liquid krypton electromagnetic calorimeter (LKr) is used to measure photon and electron showers. It consists of $\approx$10 m^3 of liquid krypton with a total thickness of 127 cm ($\approx$ 27 radiation lengths) and an octagonal shaped cross-section of $\approx$5.5 m^2. The entrance face of the calorimeter is located 11501 cm from the beginning of the decay region and 11455 cm from the location of the first η target. Immersed in the krypton are electrodes made with Cu-Be-Co ribbons of cross-section 40μm$\times$18mm$\times$127cm, extending between the front and the back of the detector. The ribbons are guided through precisely machined slots in five spacer plates located longitudinally every 21 cm which ensure the gap width stability in the shape of a $\pm$ 48 mrad accordion. The 13212 readout cells each have a cross-section of 2$\times$2 cm^2 at the back of the active region, and consist (along the horizontal direction) of a central anode at a 3 kV high voltage in the middle of two cathodes kept at ground. The cell structure is projective towards the middle of the decay region, 110 m upstream of the calorimeter, so that the measurement of photon positions is insensitive to first order to the initial conversion depth. The initial current induced on the

electrodes by the drift of the ionization is measured using pulse shapers with 80 ns FWMH and digitised with 40 MHz 10-bits FADCs [8]. The dynamic range is increased by employing four gain-switching amplifiers which change the amplification factor depending on the pulse height. The electronic noise per cell is ≈ 10 MeV. The calorimeter is housed in a vacuum insulated cryostat. The total amount of matter before the beginning of the liquid krypton volume is ≈ 0.8 radiation lengths, including all the NA48 detector elements upstream of the calorimeter. The total output of the calorimetric information is restricted to cells belonging to a region around the most energetic cells, by a "zero-suppression" algorithm. For each event, the information from 10 digitised time samples (250 ns) is read out. An iron-scintillator hadron calorimeter is located downstream of the LKr, followed by a muon veto system.

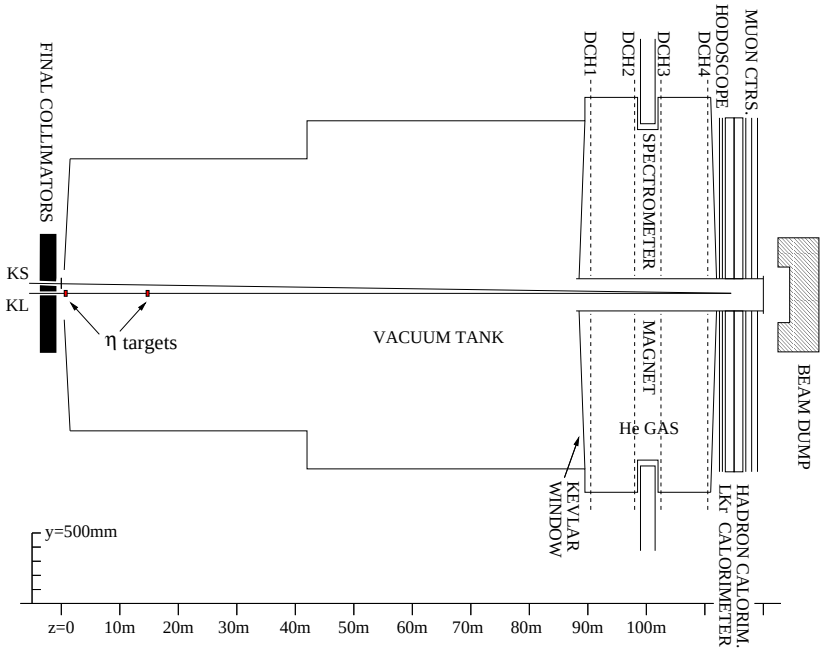

Figure 1: Layout of the main detector components.

2.4 Triggers and data sets

The trigger on multiphoton final states [9] operates on the analogue sums of signals from 2×8 cells of the LKr calorimeter in both horizontal (x) and vertical (y) orientations. The signals are digitised and summed in x and y projections. Based on these projections, the total deposited energy, the energy-weighted centre of gravity of the event and the estimated decay vertex position along the beam axis are computed.

To select $K_L \to 3\pi^0$ decays, the total energy is required to be more than 50 GeV, the radial position of the centre of gravity to be less than 15 cm from the beam axis and the decay vertex position to be less than 9 K_S-lifetimes away from the beginning of the decay region.

To select π^0 and η decays in the η runs, a cut on the total energy is applied. Events with energy above 90 GeV are taken without downscaling, events with energy between 40 and 90 GeV are downscaled by a factor 10 or 12 depending on the run period, and events with energy between 15 and 40 GeV are downscaled by a factor 4 to 6.

During the ϵ'/ϵ run in 1998 and 1999, large statistics of K_{e3} decays were collected to study the calorimeter performance. In the year 2000, the detector operated with vacuum in place of the spectrometer. During this period, data with only the K_L beam were recorded, as well as data with an η beam. These data are used for the mass measurements presented here.

3 Performance of the electromagnetic calorimeter

3.1 Reconstruction

Photon or electron showers are found in the calorimeter by looking for maxima in the digitised pulses from individual cells in both space and time. Energy and time of the pulses are estimated using a digital filter technique. The first calibration is performed using a calibration pulser system. Small drifts of the pedestal due to temperature effects are monitored and corrected for. The energy of the shower is computed accumulating the energy in the cells within a radius of 11 cm, containing more than 90% of the shower total energy (this fraction being constant with energy). The shower position is derived from the energy-weighted centre of gravity of the 3×3 central cells, corrected for the residual bias of this estimator. Shower energies are corrected for the following effects: small ($< 1\%$) variations of the energy measurement depending on the impact point within the cell, energy lost outside the calorimeter boundaries, energy lost in non-working cells

(about 0.4% of the channels), average energy lost in the material before the calorimeter (15 MeV for photons, 45 MeV for electrons), a small bias from the zero-suppression algorithm for energies below 5 GeV and small space charge effects from the accumulation of positive ions in the gap [10] which is significant only in the case of data taken with the high intensity K_L beam. Energy leakage from one shower to another is corrected in the reconstruction using the transverse shower profile from a GEANT [11] simulation. Special runs in which a monochromatic electron beam is sent into the calorimeter, taken without zero suppression, are used to check this modelling and to derive a small correction.

Fiducial cuts are applied to ensure that shower energies are well measured. These cuts include the removal of events with a shower too close to the inner beam tube or the outer edges of the LKr or falling within 2 cm of a non-working cell. Only showers in the energy range 3-100 GeV are used.

The corrections described above are the same as those applied for the ϵ'/ϵ measurement discussed in [1].

3.2 Performance from K_{e3} decays

More than 150×10^6 K_{e3} decays have been recorded during the ϵ'/ϵ data taking periods. The comparison of the electron momentum measured by the magnetic spectrometer (p) and the energy measured by the LKr (E) allows the performance of the calorimeter to be studied in detail, the resolution on the ratio E/p being $\approx 1\%$. The K_{e3} sample is first used to study and improve the cell-to-cell intercalibration of the calorimeter. After the electronic calibration, the cell-to-cell dispersion in the shower energy measurement is about 0.4%. Electrons from K_{e3} in the energy range 25-40 GeV (to avoid possible correlations between non-uniformity and non-linearity) are used to equalise the cell-to-cell energy response, requiring E/p to be the same for all cells. This is done with a statistical accuracy of about 0.15% using the 1998 data sample. Residual long range variations of the energy response over the calorimeter are expected to be smaller.

Unfolding the momentum resolution from the measured E/p resolution as a function of the electron energy, the LKr energy resolution can be obtained:

$$\frac{\sigma(E)}{E} = \frac{(0.032 \pm 0.002)}{\sqrt{E}} \oplus \frac{(0.090 \pm 0.010)}{E} \oplus (0.0042 \pm 0.0005)$$

where E is the energy in GeV. The sampling term is dominated by fluctuations in the shower leakage outside the area used to measure the energy.

The constant term arises from residual variations with the impact point, accuracy in the pulse reconstruction, residual gap variations and inter-cell calibration. The energy response is linear within about 0.1% over the energy range 5-100 GeV, as illustrated in Figure 2 which shows the average value of E/p as a function of the electron energy. The measured small variation of E/p as a function of energy is applied as a correction to the photon energies.

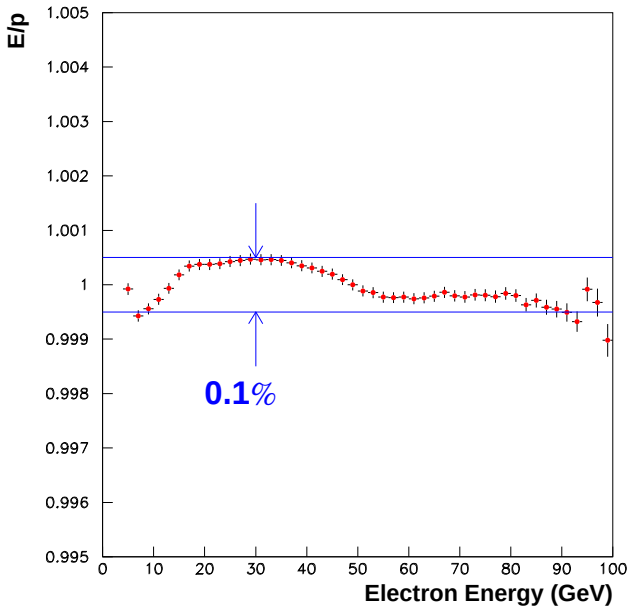

Figure 2: Limit to the non-linearity of energy measurement from K_{e3} decays

The comparison of the reconstructed electron position using the calorimeter with that of the extrapolated track allows the position measurement of the LKr to be adjusted and its transverse size scale to be checked with an accuracy of 2.5×10^{-4}. The position resolution of the calorimeter is better than 1.3 mm above 20 GeV.

3.3 Study of systematic effects using π^0 decays

Using the large sample of π^0 decays to two photons produced during the η runs, the systematic effects in the calorimeter measurement can be estimated. From the known target positions, the π^0 mass can be reconstructed

from the measured photon energies and positions at the LKr. Figure 3 shows the relative variation of the reconstructed π^0 mass as a function of several variables: photon impact position, π^0 energy, maximum and minimum photon energy. Significant non-uniformities in the energy response would lead to a visible variation of the π^0 mass with the photon impact point. Non-linearities in the energy response would lead to drifts in the reconstructed mass as a function of the energy. As can be seen in Figure 3, the π^0 mass is stable to $\approx 0.1\%$, except in the energy region $E_\gamma < 6$ GeV, where stronger effects can be seen. However, this energy region is not used in the analysis of symmetric $3\pi^0$ decays, where the photon energies are in the 8 to 37 GeV range. The π^0 sample is also used for the 2000 data to improve the 1998 K_{e3} intercalibration, by equalising the reconstructed π^0 mass value as a function of the photon impact cell. The dispersion of the correction coefficients is about 0.1%.

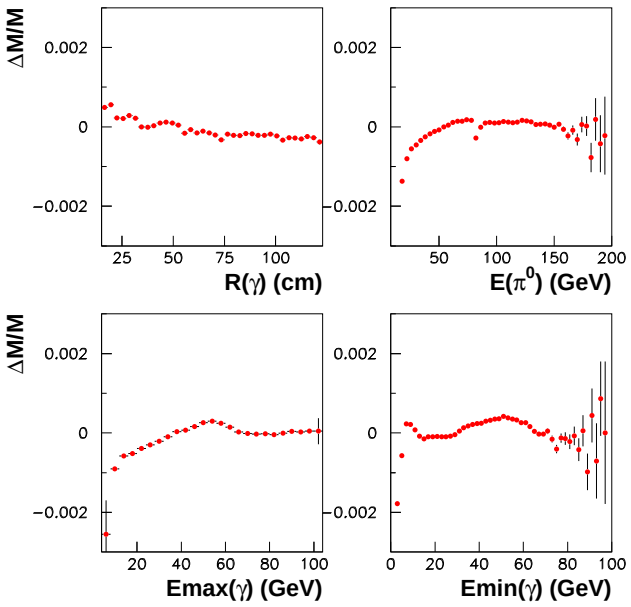

Figure 3: Relative variation of the reconstructed π^0 mass, as a function of the impact radius of photons, total π^0 energy and maximum and minimum energy of the two photons

The non-linearities in the energy response can be parameterised as:

$$\frac{\Delta E}{E} = \frac{\alpha}{E} + \beta E + \gamma r \tag{1}$$

where E is the photon energy and r the impact radius over the calorimeter. From the $\pi^0 \to \gamma\gamma$ data, α can be constrained to be within $\pm$ 10 MeV, β within $\pm 2 \times 10^{-5}$ GeV^{-1} and γ within $\pm 10^{-5}$ cm^{-1}.

4 η and K^0 masses measurement

4.1 Selection of $3\pi^0$ decays

To select $3\pi^0$ decays, any group of six showers within $\pm$5 ns of their average time is examined. No other shower above 1.5 GeV should be present within a $\pm$ 3 ns time. The minimum distance between photon candidates is required to be greater than 10 cm. The total energy is required to be in the range 70-170 GeV for K_L, and 70-180 GeV for η decays. Using the six photons, the decay vertex position along the beam axis is computed assuming the K^0 or the η mass [1]. The resolution is $\approx$ 50 cm. In the η case, this position is required to be consistent with the position of one of the two targets within 400 cm. In the K_L case, the decay vertex position should be less than 6.5 K_S lifetimes downstream of the beginning of the decay region. Using this decay vertex, the invariant mass of any pair of photons is computed. A χ^2 like variable is computed comparing the masses of the three pairs to the nominal π^0 mass. The typical π^0 mass resolution is around 1 MeV and is parametrised as a function of the lowest energy photon. The pairing with the smallest χ^2 is selected. To remove any residual background (from events with a π^0 Dalitz decay for example), a loose χ^2 cut is applied. The correct π^0 pairing is selected by this method in 99.75% of the events, and the residual bias on the mass result induced by wrong pairing is completely negligible. This procedure selects 128×10^6 $K_L \to 3\pi^0$ candidates and 264×10^3 $\eta \to 3\pi^0$ candidates in the data from the year 2000.

To minimise the sensitivity of the measurement to residual energy non-linearity, configurations in which the photons have comparable energies are selected using the following cut on each photon energy:

$$0.7 < \frac{E_\gamma}{\frac{1}{6}E_{tot}} < 1.3$$

[1] The assumed mass values at this stage are only used to perform a loose selection, and they do not affect the final mass measurement

where E_γ is the energy of the photon and E_{tot} the sum of the energies of all photons. This cut leaves a sample of 655×10^3 K_L decays and 1134 η decays. The events are then subjected to the mass reconstruction described in section 1. In these computations, photon positions are evaluated at the position of the maximum of the shower in the calorimeter, to account correctly for deviations of photon directions from the projectivity of the calorimeter. The same procedure is applied to Monte-Carlo samples of K_L and η decays, following the same reconstruction and analysis path, to check for any bias in the procedure. The simulation of the calorimeter response is based on a large shower library generated with GEANT.

4.2 Results and cross-checks

The distributions of the differences of the reconstructed η and K^0 masses from the world average masses[2] are shown in Figure 4. The average values of these distributions are 550 ± 30 keV/c^2 for the η sample and -43 ± 1 keV/c^2 for the K_L, where the errors quoted are only statistical. When the same analysis is applied on the Monte-Carlo samples, the shifts observed between the input mass and the average reconstructed mass are 7 ± 5 keV/c^2 for the η case and $+4 \pm 3$ keV/c^2 for the K_L sample. This shows that residual bias from reconstruction and resolution effects are small.

The sensitivities to the non-linearities discussed in the previous section are estimated changing the parameters α and β in Equation 1 and recomputing the reconstructed masses in the Monte-Carlo samples. The uncertainties associated with the allowed range of α and β are ± 2 keV/c^2 each on both the K^0 and η masses. This small level of uncertainty is made possible by the use of symmetric decay configurations. The uncertainty associated with residual non-uniformity in the calorimeter response (parameter γ) is evaluated by comparing the reconstructed masses with and without the final correction derived from the 2000 π^0 data and is found to be ± 23 keV/c^2 for both the η and K^0 masses. This is essentially equivalent to varying the parameter γ within $\pm 10^{-5}$ cm^{-1}.

The reconstruction of the mass is also sensitive to the effect of energy leakage from one shower to another. The uncertainty associated with the shower profile parameterisation is taken to be the difference between the shower profile predicted by GEANT and the profile measured with electron data. The uncertainty associated with the Monte-Carlo modelling of the residual reconstruction bias is taken to be half the size of this bias. This leads

[2] The values are 0.547300 GeV/c^2 for the η mass and 0.497672 GeV/c^2 for the K_L mass

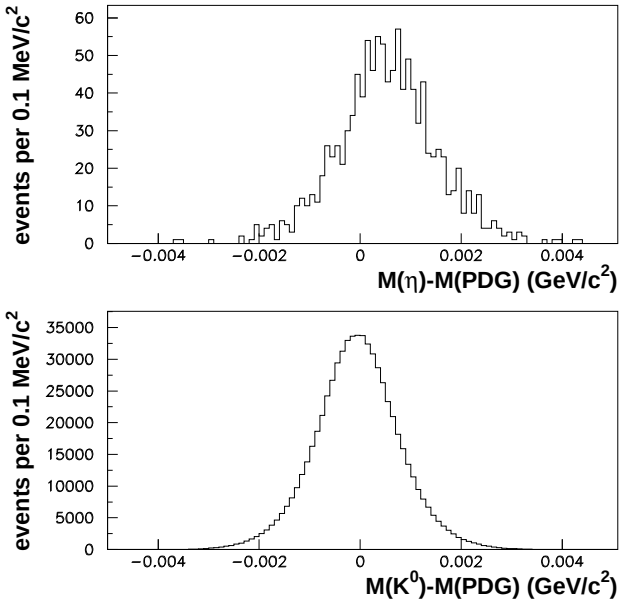

Figure 4: Reconstructed masses from $3\pi^0$ decays, from the η sample (top) and the K_L sample (bottom)

to a systematic error on the mass of ± 33 keV/c^2 for the η and ± 20 keV/c^2 for the K^0.

The uncertainty in the photon position measurement is estimated using the nominal calorimeter geometry without the corrections derived from K_{e3} data. The corresponding uncertainty in the η mass is ± 9 keV/c^2, and ± 5 keV/c^2 on the K^0 mass (Because there is no collimation for the η case, the centre of gravity of the events is spread over the full calorimeter, unlike the K_L case, and this enhances the sensitivity to this effect).

Finally, the energy response has non-Gaussian tails arising mostly from hadron production at the early stages of the shower. To study the sensitivity to this effect, these tails were parameterised from K_{e3} and π^0 data and introduced in the Monte-Carlo. The effect of using this parameterisation in the Monte-Carlo is a change of 2 keV/c^2 for both the η and K^0 cases. This change is taken as the estimate of the uncertainty.

The effect of accidental activity from the K_L beam has been investigated

and found to be negligible on the reconstructed kaon mass.

Combining the various contributions in quadrature, the total systematic error amounts to ± 41 keV/c^2 for the η mass and ± 31 keV/c^2 for the K^0 mass. Correcting the data for the small observed Monte-Carlo shifts, the following values are thus obtained:

$$M_\eta = 547.843 \pm 0.030_{stat} \pm 0.005_{MC} \pm 0.041_{syst} \text{ MeV/c}^2$$
$$M_{K_L} = 497.625 \pm 0.001_{stat} \pm 0.003_{MC} \pm 0.031_{syst} \text{ MeV/c}^2$$

Many cross-checks of this measurement have been made. The stability of the reconstructed masses as a function of several variables has been investigated and found to be within the quoted systematic errors. The same value of the mass is found for η originating from both targets. Repeating the procedure on the lower statistics samples collected in 1999 has yielded consistent results. For the neutral Kaon case a similar analysis as for $3\pi^0$ has been performed on $2\pi^0$ decays, using events collected in the ϵ'/ϵ runs and also, separately, those obtained at the same time as the η decays. The agreement obtained is particularly significant because we have found that the effect of the dominant systematic uncertainty, which originates from energy leakage effects, is actually anticorrelated between the $2\pi^0$ and the $3\pi^0$ samples.

As an alternative to using symmetric decays for the K^0 mass measurement, events have been selected by an algorithm which requires minimum sensitivity to energy non-linearities. This gives a higher statistics sample, spanning a wider range of energies, and the K^0 mass measurement agrees to better than 10 keV/c^2.

Relaxing the cut on the symmetry of the decay and asking $E_\gamma > 6$ GeV and at least 25 cm separation between photons, the reconstructed masses move by -9 keV/c^2 for the η and -10 keV/c^2 for the K^0, while the total systematic error is increased by almost a factor two because of the much stronger sensitivity to energy non-linearities.

The K_L to $3\pi^0$ decays have also been analysed using a kinematical fit. In addition to four energy and momentum constraints for the decay, the three photon pairs were constrained to have invariant masses equal to the π^0 mass. The linearised constraints equations were expressed in terms of two impact coordinates and energy of each photon in the calorimeter. In the fitting procedure the K^0 mass as well as its energy and decay vertex position were determined. Typically the fit converged after 2-3 iterations. The measurement errors were slightly adjusted to have good stretch functions and the resulting fit probability distribution was flat except for an

enhancement below 5%. Using the fitted mass and its error, the K^0 mass was determined from the weighted average in the $\pm 5\,\mathrm{MeV/c^2}$ mass window around the world average mass. This method has somewhat different sensitivities to systematic effects than the method discussed previously. The results from the two methods were compared for various cuts on the event selection, and they were found to agree within ± 10 keV, which is within the quoted systematic uncertainty.

Another independent cross-check of systematic effects can be performed using $\pi^0, \eta \to \gamma\gamma$ produced at the targets. Using these two different decays, the ratio of the η mass to the π^0 mass can be computed. The selection of the events can be done such as to have either (a) the same energy for the π^0 and η, but different separation between the photons (by a factor 4 which is the mass ratio) and thus different systematics in the energy leakage from one cluster to another, or (b) the same distance between the two photons but then energies differing by a factor 4 and thus a sensitivity to the energy non-linearity. Symmetric $\gamma\gamma$ decays are selected requiring $0.8 < \frac{E_\gamma}{E_{tot}} < 1.2$. To reduce background, events with energy leakage in the hadron calorimeter are removed. The selected range for the η energy is 90-120 GeV. In case (a) the same range is used for the π^0 events, while in case (b) the energy range for the π^0 is 22.5-30 GeV. The values obtained for the η mass are $M(\eta) = 547.80 \pm 0.14$ MeV/c^2 using the selection (a) and $M(\eta) = 548.15 \pm 0.35$ MeV/c^2 for selection (b). The errors quoted include the effect of all the systematic uncertainties discussed above. In case (a), the dominant uncertainty is the systematic uncertainty on the correction of energy leakage from one cluster to the other. In case (b), it is the systematic uncertainty associated with energy non-linearity. These measurements suffer from larger sensitivities to systematic effects than the one using $3\pi^0$ decays, but within the uncertainties, there is good agreement between the results, thus giving a further cross-check that systematic effects are under control.

5 Conclusions

From the $3\pi^0$ symmetric decay configuration, the following mass values are obtained:

$$M_\eta = 547.843 \pm 0.051 \text{ MeV/c}^2$$

$$M_{K^0} = 497.625 \pm 0.031 \text{ MeV/c}^2$$

The K^0 mass is consistent with the present world average within 1.1 standard deviations, with a similar uncertainty. The uncertainty on the

η mass is about 2.4 times smaller than the current world average uncertainty, while the eta mass differs from the world average by about 0.1%, corresponding to 4.2 standard deviations.

Acknowledgements

We would like to warmly thank the technical staff of the participating laboratories and universities for their dedicated effort in the design, construction, and maintenance of the beam, detector, data acquisition and processing.

References

[1] A. Lai et al., EPJ C 22 (2001) 231.

[2] Review of Particle Physics, D. E. Groom et al., EPJ C 15 (2000) 1.

[3] L. M. Barkov et al., SJNP 46 (1987) 630.

[4] F. Plouin et al., Physics Letters B 276 (1992) 526.

[5] B. Krusche et al., Z. Physics A 351 (1995) 237.

[6] C. Biino et al., CERN-SL-98-033(EA).

[7] D. Bédérède et al., Nucl. Instr. and Methods A 367 (1995) 88.
I. Augustin et al., Nucl. Instr. and Methods A 403 (1998) 472.

[8] B. Hallgren at al., Nucl. Instr.and Methods A 419 (1988) 680;
C. Cerri, Proc. VI Int. Conf. on Calorimetry in HEP, Frascati 1996,
A. Antonelli et al. ed., Frascati Physics Serie 6 (1996) 841;
G. Martin-Chassard et al., ibid. 799.

[9] G. Barr et al., CERN-EP/2001-079 to be published in Nucl. Instr. and Methods A

[10] S. Palestini et al., Nucl.Ĩnstr.ãnd Methods A 421 (1999) 75.

[11] GEANT Detector Description and Simulation Tool, CERN Program Library Long Writeup W5013 (1994).